Volume 16, Number 5, 2023. pp. 563-578

Jordan Journal of Physics

ARTICLE

Origin of the Magnetic-Optical Properties of Palladium Compounds, an Ab Intio Study

Ouarda Benamara[a], **Ahmed Boufelfel**[b], **Kamal Zanat**[b] and **Wissam Selatenia**[b]

[a] *Guelma Laboratory of Physic, University 8 May 45 Guelma, Algiers.*
[b] *Guelma Laboratory of Physic, University 8 May 45 Guelma, Algiers.*

Doi: https://doi.org/10.47011/16.5.7
Received on: 16/01/2022; *Accepted on: 06/06/2022*

Abstract: The structural, magnetic, and magneto-optical properties of the PdM (M=Fe, Co, Ni) alloy are investigated using first-principles calculations with the exciting code. The study employs the full potential linearized augmented plane wave method (FP-LAPW) based on density functional theory (DFT). The exchange-correlation energy is described in the generalized gradient approximation developed by Perdew-Burke-Ernzerhof (PBE-GGA). The calculated lattice parameters are in good agreement with theoretical and experimental results. The magnetic properties reveal a ferromagnetic stability phase for all compounds. Additionally, the total (TDOS) and partial (PDOS) density of states, along with the band structure, indicate that PdM (M = Fe, Co, Ni) exhibits metallic behavior. The total and local magnetic moments are investigated. We conducted a study on the polar magneto-optical Kerr effect and calculated Kerr spectra. The microscopic origins of the peaks found in Kerr's angle are interpreted as interband transitions, primarily arising from the states (d to d) in the PdNi and (S to d) in the PdFe and PdCo alloys.

Keywords: P-MOKE, DFT, GGA-PBE, Intermetallic.

1. Introduction

Science and technology have been developing magnetic materials for centuries. Several of these materials are exploited through the most innovative forms of application, and their properties are utilized in a wide range of technical fields [1-4], including information storage and telecommunications [5].

Magnetic intermetallic compounds occupy a privileged position in the field of materials science due to their many applications [6-8]. The most common intermetallic compounds are those based on the alloying of transition metals such as iron, cobalt, and nickel with palladium, PdM (M = Fe, Co, Ni) [9, 10]. These compounds are of fundamental interest for their high uniaxial anisotropy of about 107 MJ/m3, which results from their natural superlattice structure. In addition, L_{10} nanoclusters have high potential as cluster-assembled granular films for 1 Tb/in^2, which have been extensively studied during the last decades for their application in various industries, particularly in electronics and electrical engineering, such as in motors or electrical transformers.

L_{10}-ordered structures such as Pd–Co, FePd, and Ni-Pd are promising materials for this application [11] because of their high uniaxial magnetic anisotropy energies.

Previous theoretical studies, based on first-principle calculations [12, 13] have contributed to a deeper understanding of the magnetic properties of these materials and the origin of giant magnetic moments at Co sites [14, 15].

Corresponding Author: Ouarda Benamara **Email**: Benamara_war@yahoo.fr

Iron palladium (FePd) alloys have demonstrated substantial magnetic-field-induced strains[16].

These alloys play a crucial role in data storage for magneto-optical recording [17], currently being a highly applicable technique for erasable optical recording on perpendicular magnetized media. The readout of such media involves using the polar magneto-optic Kerr effect (P-MOKE) [18]. Martın-Gonzalez and Visnovsky have studied the magneto-optical properties of FePd and PdNi, respectively [19-21].

In this paper, motivated by the above facts, we aim to find the microscopic origin of the polar magneto-optical (MO) Kerr effect (P-MOKE) spectra within the framework of density functional theorem (DFT), following a comprehensive analysis of the structural, magnetic, and MO properties of PdM compounds with M = (Fe, Co, Ni).

2. Computational Method

In this article, we study the structural, magnetic, and magneto-optical properties of PdM (M = Fe, Co, Ni) compounds within the framework of the density functional theory (DFT) [22, 23]. The calculations are performed using the augmented plane wave method linearized with full potential (FP-LAPW), implemented in the "Exciting" code [24]. The generalized gradient approximation (GGA-PBE), developed by Perdew, Burk, and Ernzerhorf [25], is employed to predict structural properties.

The PdM (M = Fe, Co, Ni) compounds crystallize in a tetragonal structure L_{10} with space group 123 P4/mmm. The atomic positions for Pd are (0,0,0) and (1/2.1/2.0), while for M=(Fe, Co, Ni), they are (0.1/2,1/ 2), (1/2,0,1/2) as presented in Fig. 1.

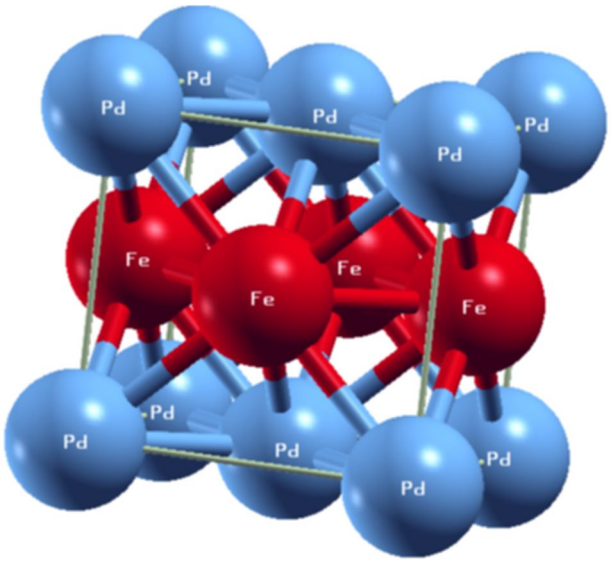

FIG. 1. Crystalline structure L10 of PdM; M = (Fe, Co, Ni).

The density of k-points was set to 12x12x12 for sampling the Brillouin zones. A plane wave cutoff of rgkmax = 9 was utilized, and an energy convergence limit was set to 0.0001Ry.

3. Results and Discussions

3.1 Structural Properties

We performed several self-consistent calculations to optimize the total energy as a function of the unit cell volume, for each given volume.

The results obtained for total energy as a function of volume were subsequently fitted to a semi-empirical equation of state. In the present work, we have used the Birch-Muringhan equation [26] given by:

$$E(V) = E_0 + \frac{9B_0V_0}{16}\left[V_0/V^{2/3} - 1\right]^3 \acute{B} + \left[V_0/V^{2/3} - 1\right]^2 + \left[6 - 4(V_0/V)^{2/3}\right] \quad (1)$$

where E_0 and V_0 are, respectively, the total energy and the pressure equilibrium volume at temperature zero.

The compressibility modulus is determined by the equation:

$$B = v\frac{\partial^2 E}{\partial V^2} \quad (2)$$

The results for the alloys PdFe, PdCo, and PdNi are shown in Fig. 2. The figure

encapsulates the evolution curves of the total energy of the system as a function of volume obtained by the GGA-PBE approximation.

In Table 1, we have collected all the equilibrium quantities of the PdM alloy (M = Fe, Co, Ni). This includes essential parameters such as the lattice constant a_0, the compression modulus B, and its derivative B', all calculated *ab initio* using the GGA-PBE exchange-correlation potential approximations. Additionally, the table incorporates available experimental values and other *ab initio* calculations to facilitate comparison.

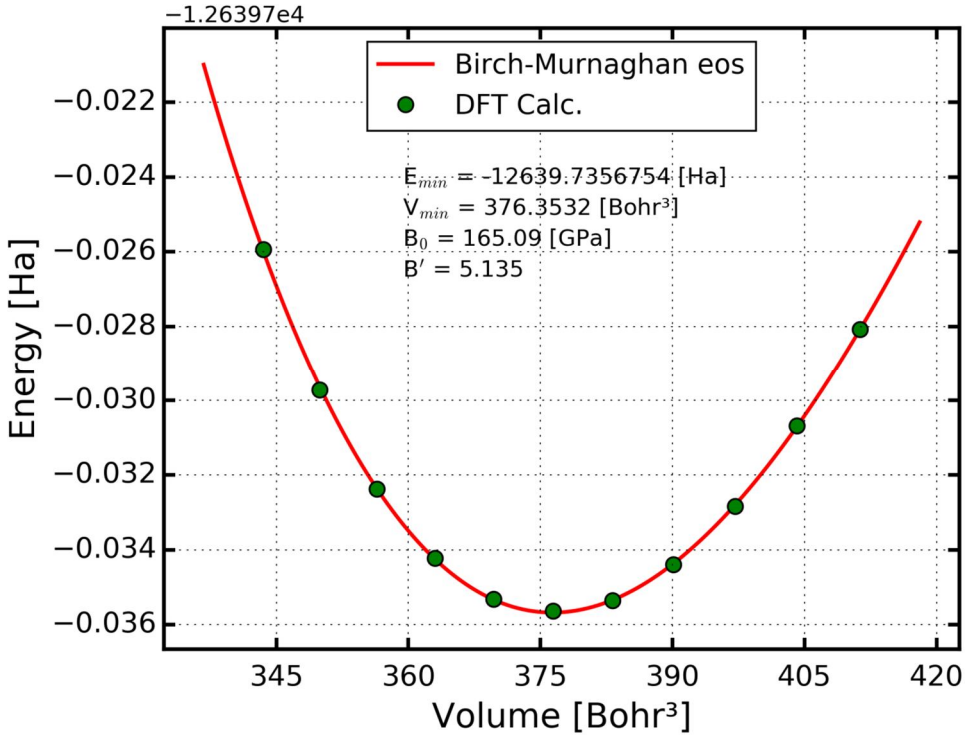

(a)

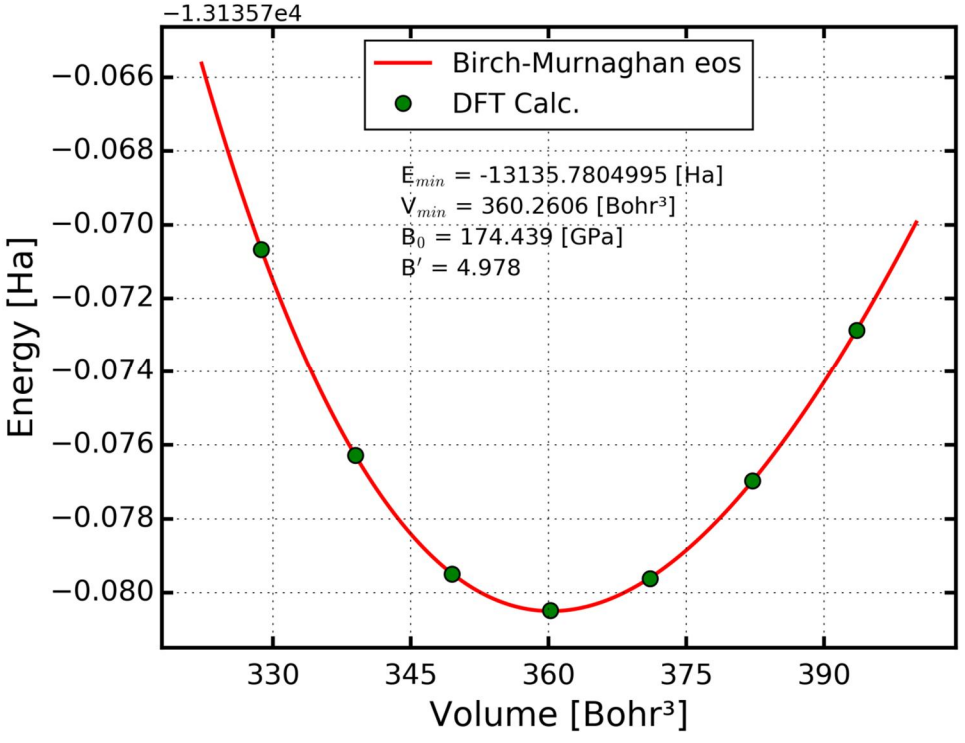

(b)

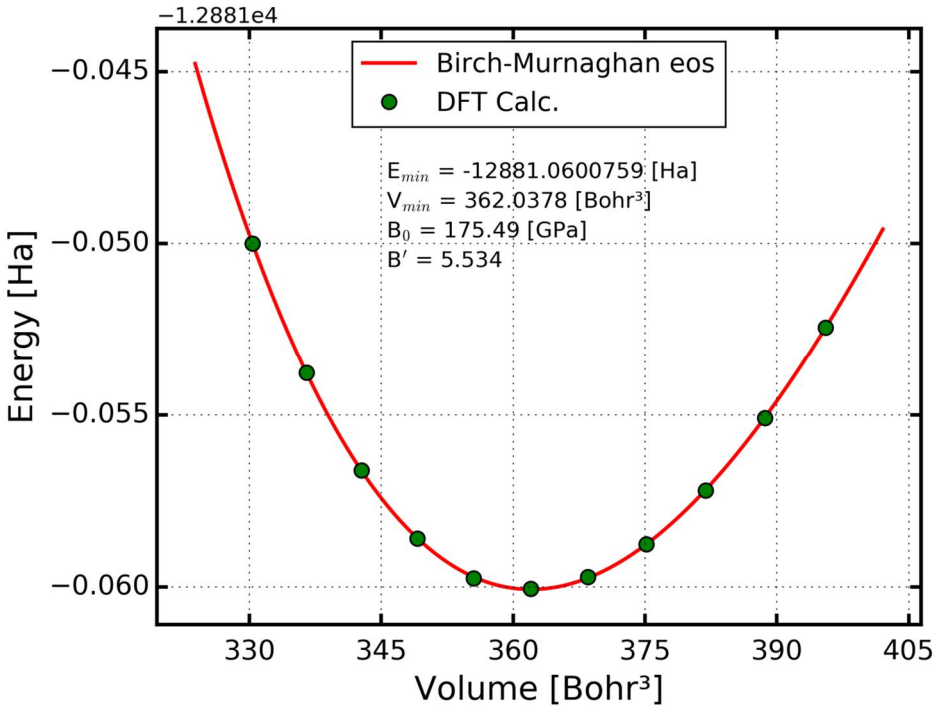

(c)

FIG. 2. The evolution of the total energy of the system as a function of the volume of: (a) PdFe, (b) PdNi, (c) PdCo.

TABLE 1. Structural properties of PdM (M = Fe, Ni).

	a (A°)	c/a (A°)	B (GPa)	B'
PdFe	3.85 3.85[a] 3.84[b] 3.85[c] 3.85[d] 3.89[e]	0.97 0.97[a] 0.96[b] 0.97[c] 0.97[d] 0.96[e]	165.09	5.135
PdCo	3.78 3.79[f]	0.99 0.97[f]	175.49	5.534
PdNi	3.85 3.81[g] 3.76[h] 3.75[i]	0.93 0.93[g] 0.92[h] 0.92[i]	174.439	4.978

a: Expt [27] ; b: Expt [28]; c: Expt [29]; d: Theor [30]
e: Theor [31]; f: Expt [32]; g: Expt [33]; h: Theor [34]; i: Theor [35].

From Table 1, it can be deduced that the results obtained from the value of the lattice parameter are in good agreement with the experimental and theoretical data. So, the results are close to each other.

3.2 Magnetic Properties

The results of the total (TDOS) and partial (PDOS) density of state for PdFe, PdCo, and PdNi alloys, with polarized spin projected between -0.3 Ha and 0.3 Ha and determined by the GGA-PBE, are illustrated in Figs. 3, 4, and 5, respectively. The level of fermi is taken as the origin of the energies and represented by a dotted line.

From the TDOS and PDOS curves of the PdM alloy (M = Fe, Co, Ni), several observations are evident.

The total density results show the existence of two regions:

- A region between -0.3 Ha and 0 Ha below Fermi level, corresponding to the valence band, is dominated mainly by the contribution of the d states of the two atoms that make up this compound.
- A region between 0 Ha and 0.4 Ha above Fermi level, corresponding to the conduction band, is formed by a mixture of the s, p, and d states of the two atoms that make up this compound.

a)

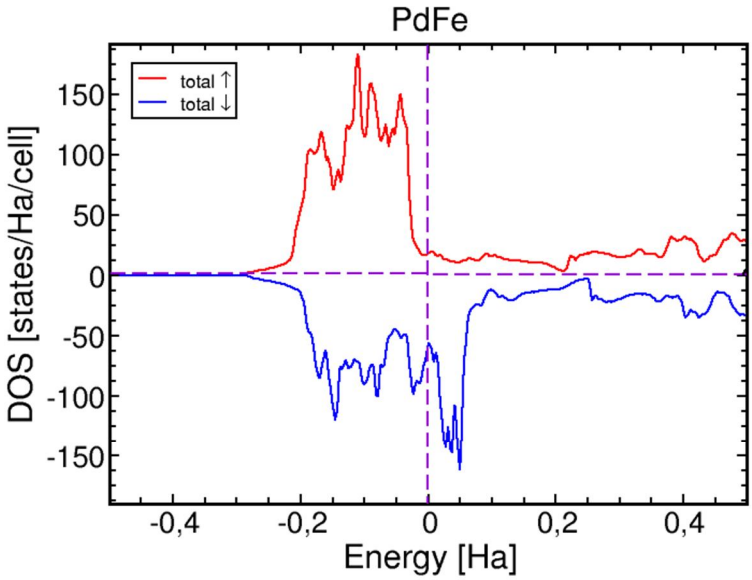

b)

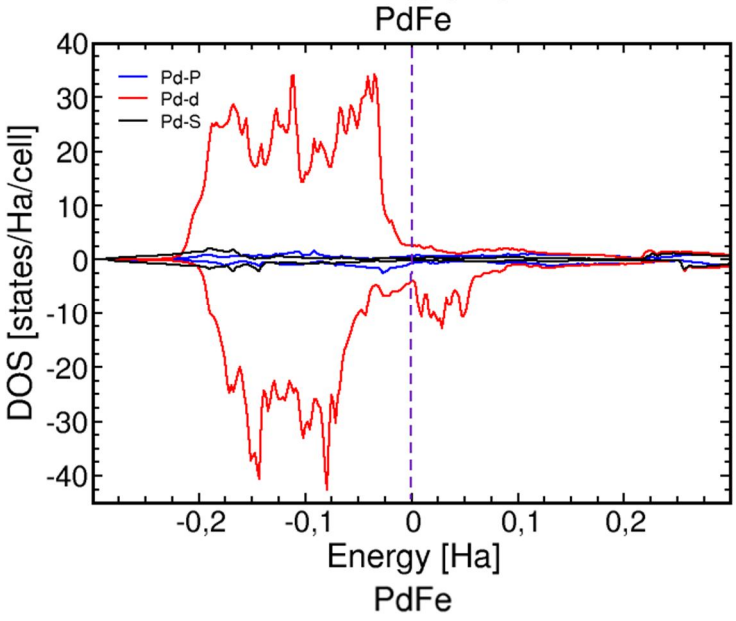

c)

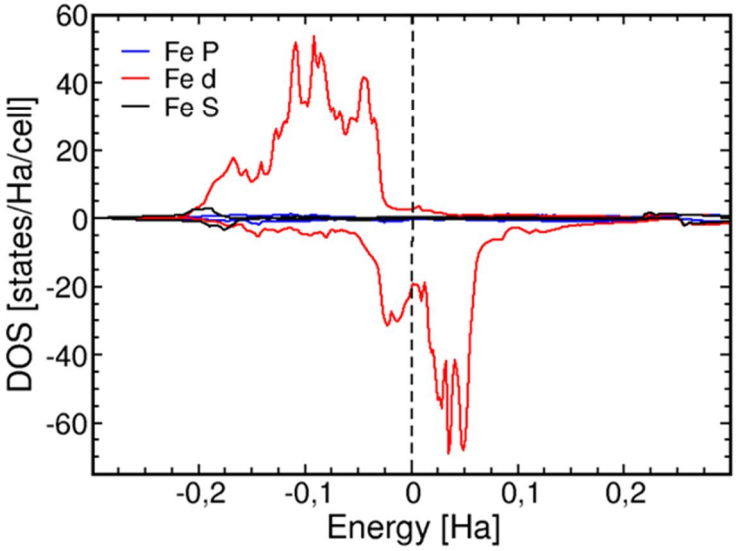

FIG. 3. **(**a) The total state density (TDOS) of PdFe, (b) the partial state density of Pd, (c) the partial state density of Fe.

a)

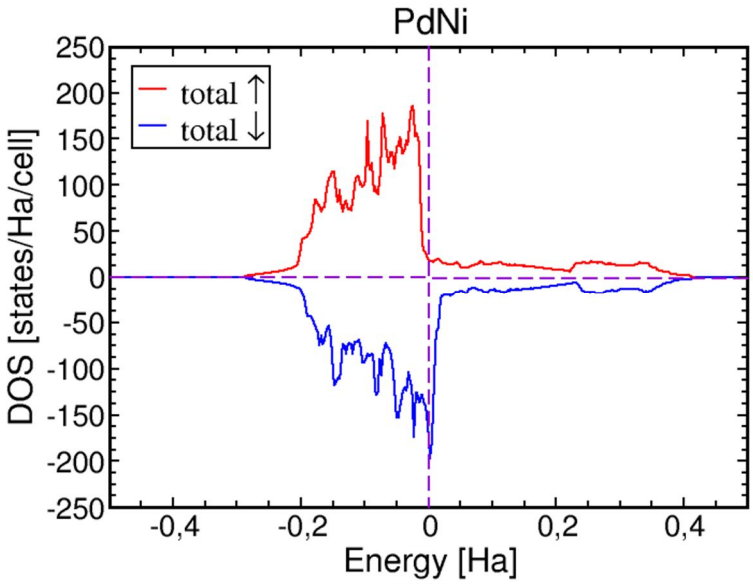

b)

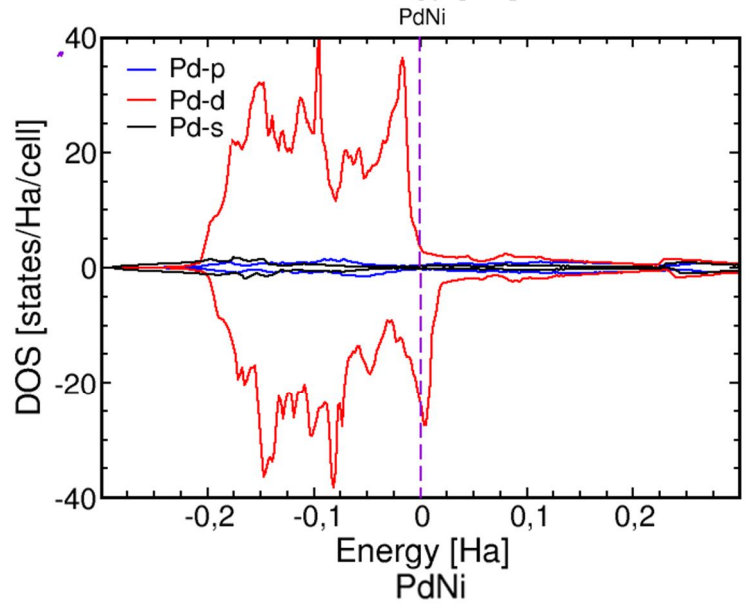

c)

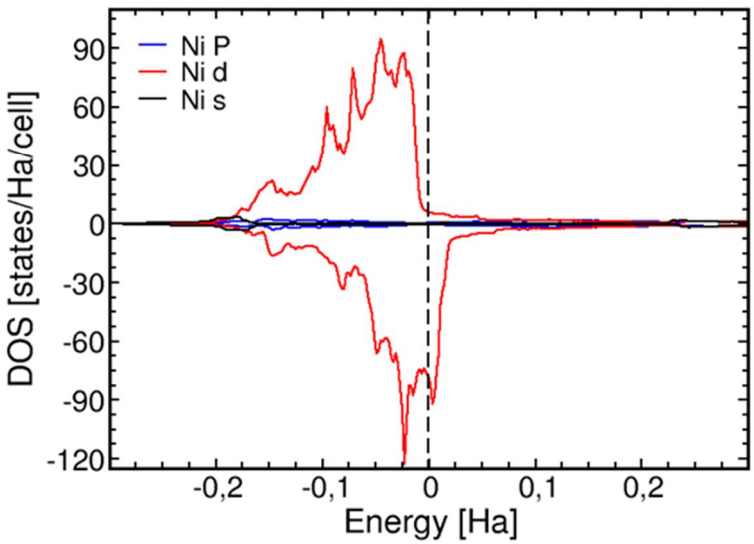

FIG. 4. (a) The total state density (TDOS) of PdNi, (b) the partial state density of Pd, (c) the partial state density of Ni.

a)

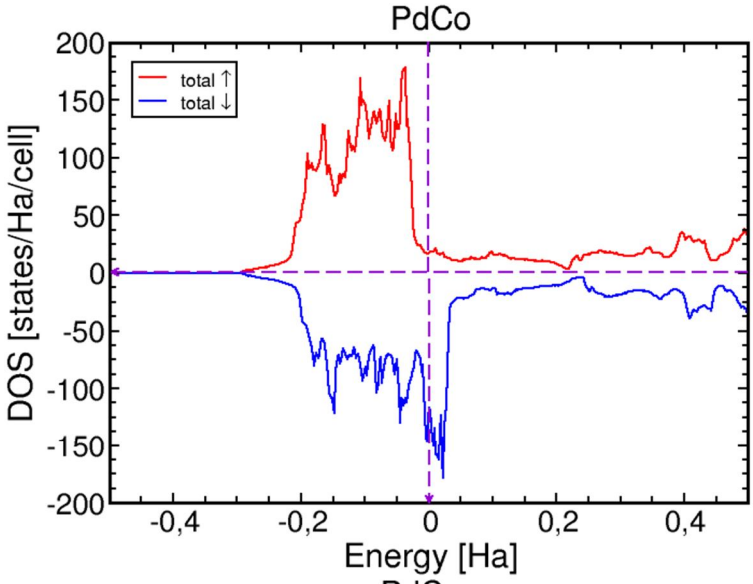

b)

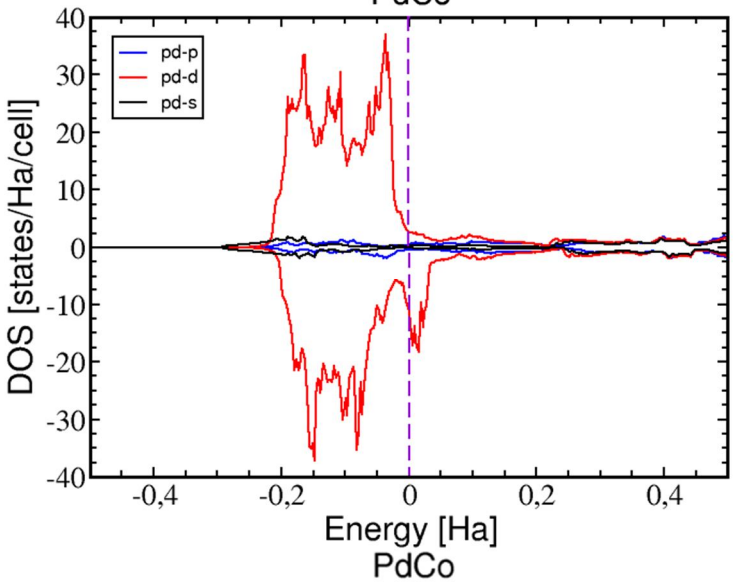

c)

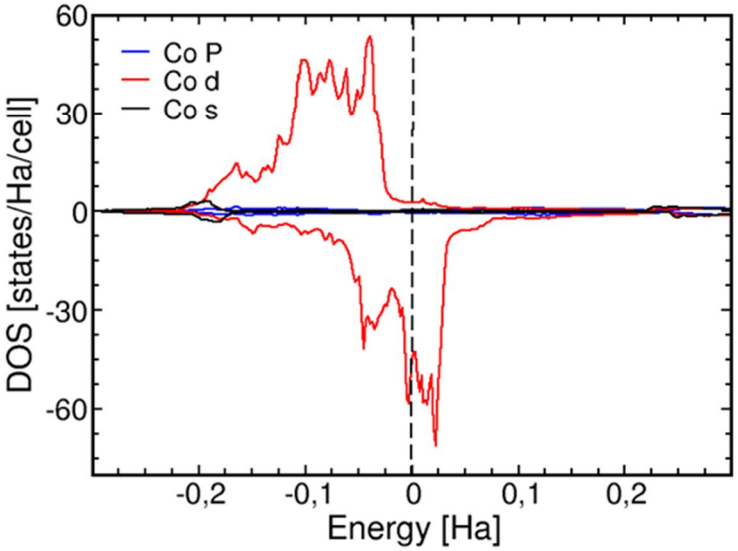

FIG. 5. (a) The total state density (TDOS) of PdCo, (b) the partial state density of Pd, (c) the partial state density of Co.

In addition, and for more clarity, we have also calculated the energy bands of the three compounds (Fig. 6). The absence of a band gap is evident for both spin-up and spin-down directions in the vicinity of the Fermi level, which confirms the metallic nature of the PdM alloy (M = Fe, Co, Ni).

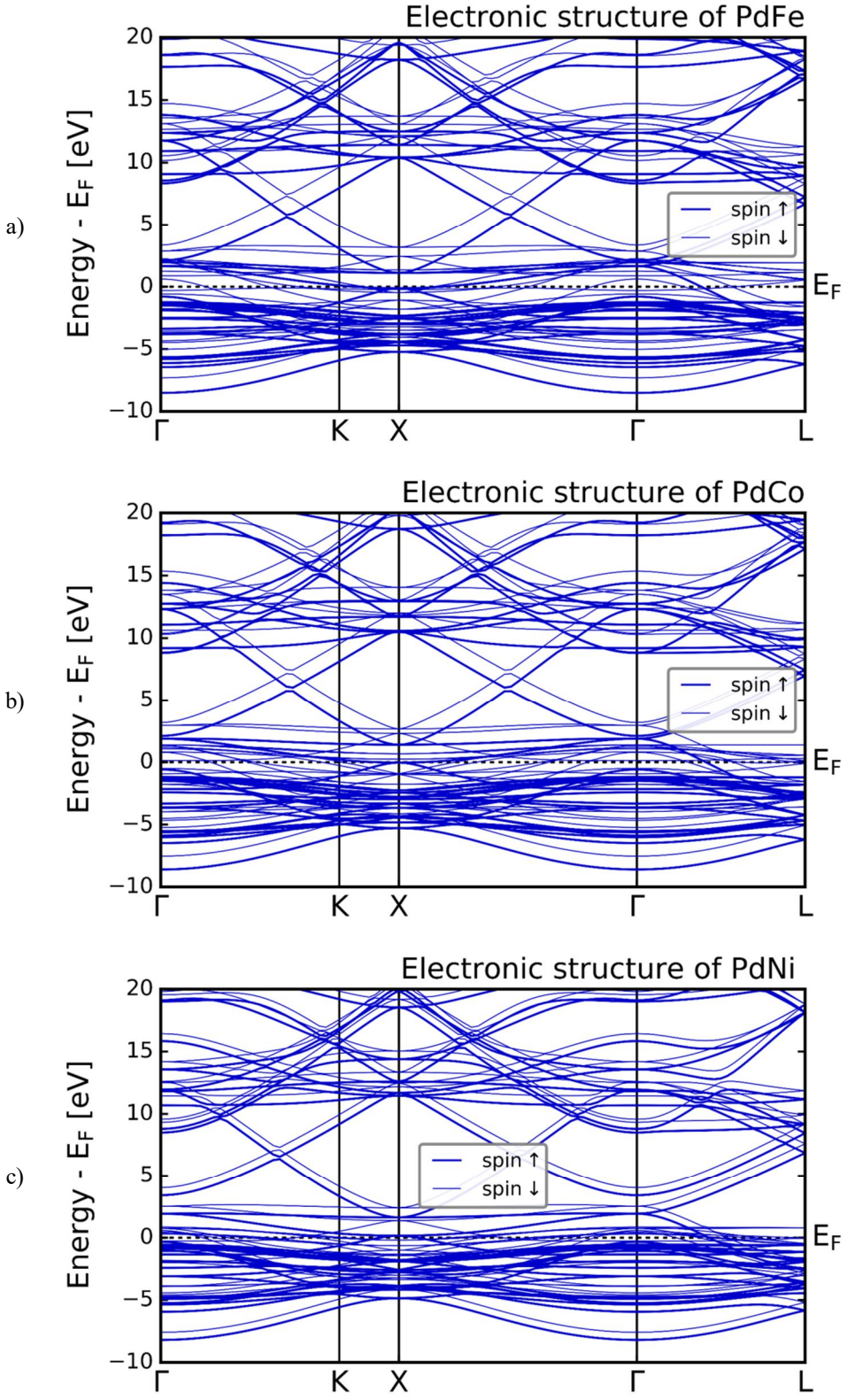

FIG. 6. Band structure of (a) PdFe, (b) PdCo, (c) PdNi.

To prove the magnetization state at which the ground-state phase stabilizes at absolute zero temperature (0 K) [36, 37], we have calculated the three phases of magnetism, antiferromagnetic G-type phase (AF), paramagnetic (PM), and the ferromagnetic (FM) phase (see Fig. 7).

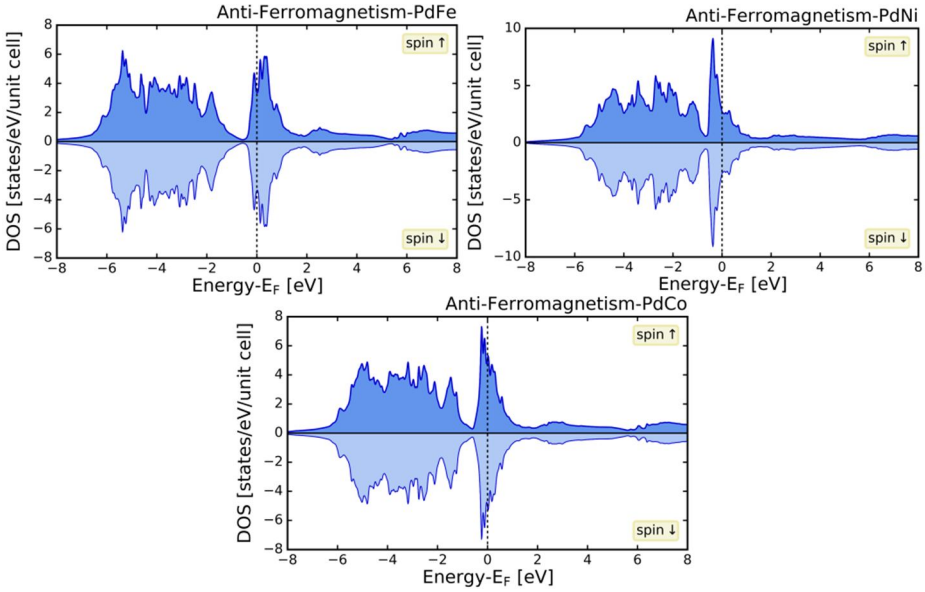

a)

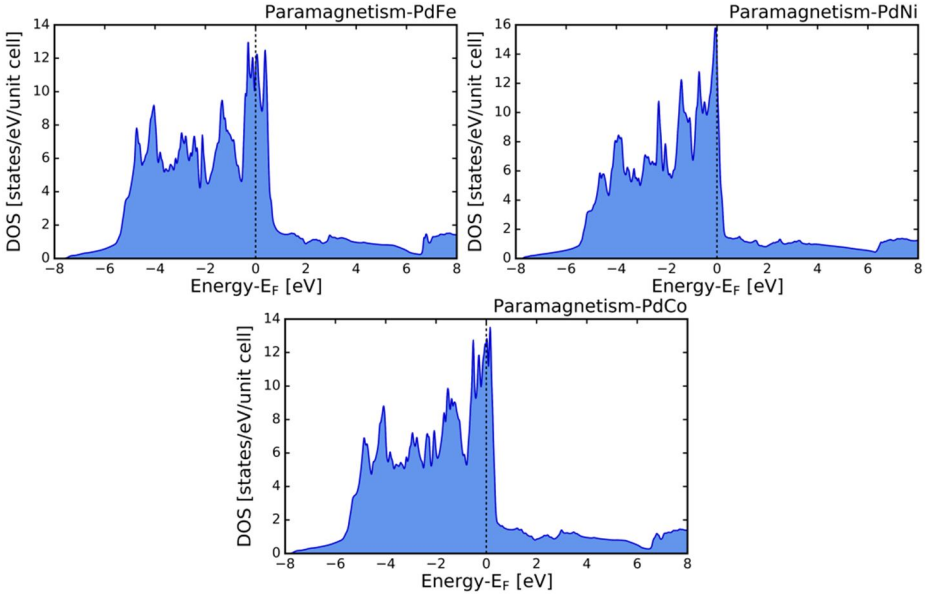

b)

FIG. 7. The total density of state in (a) the antiferromagnetic phase and (b) the paramagnetic phase for PdFe, PdNi, and PdCo compounds.

In the PM calculations, all compounds have a large DOS peak at the Fermi level, which marks the Stoner instability of the paramagnetic phase in favor of the magnetic phases.

We consider only one AF configuration, the G-type phase, in addition to the ferromagnetic (FM) phase. Total energy calculations for these magnetic phases (AF G-type and FM) demonstrate that they are more stable than the PM (see Table 2). We found that the FM phase is more stable than, at least, the AF G-type configuration.

Moreover, the AF DOS reveals that the large DOS at E_F still exists, which reflects and confirms the stability of the FM order against the considered AF order.

The total energies have provided clarity on the stable structure, revealing that the ferromagnetic configuration is stable for all compounds.

Table 3 groups together the values of the total and local magnetic moments calculated of the PdM alloy (M = Fe, Co, Ni)

The values of the total magnetic moment listed in Table 3, calculated using the GGA-PBE approximation in our case, agree with the experimental results for the PdFe, PdNi, and PdCo alloys.

TABLE 2. Antiferromagnetic (AF), Paramagnetic (PM), and ferromagnetic (FM) energies of PdM alloys in Hartree units.

	E_{PM}	E_{AFM}	E_{FM}
PdFe	-12639.6675836	-12639.7015904	-12639.7356387
PdCo	-12881.0211819	-12881.0175115	-12881.0600499
PdNi	-13135.7750824	-13135.7653212	-13135.7809767

TABLE 3. Total and partial magnetic moments of compounds PdM: M = (Fe, Co, Ni), with μ_B units.

	M_{pd}	M_M	M_{pdM}
PdFe	0.35; 0.35^a ;0.30^b ;0.34^c	2.97 ; 2.85^a;3.03^b ;2.95^c	3.33 3.29^c
PdCo	0.36 ; 0.35^a ;0.37^c	1.91 ;1.97^a ;1.90^c	2.28 2.28^c
PdNi	0.30 $\mathbf{0.28^c}$	0.76 ;$\mathbf{0.73^c}$	1.07 $\mathbf{1.1^a}$;$\mathbf{1.01^c}$

a: Expt [38], b : Theor [30], c : Theor [39].

3.3 Magneto-optical Properties

The Kerr effect in its polar geometry is the most used in theoretical and experimental studies thanks to its numerous technological applications, including magnetic recordings and reading.

Since all magneto-optical properties are directly related to optical conductivity, in a tetragonal system in which the magnetization is oriented along the z-axis, the conductivity tensor [41] is given by the expression:

$$\sigma(\omega) = \begin{bmatrix} \sigma_{xx} & \sigma_{xy} & 0 \\ -\sigma_{xy} & \sigma_{yy} & 0 \\ 0 & 0 & \sigma_{zz} \end{bmatrix} \quad (3)$$

Flat light, reflected off a thin film metal surface, becomes elliptically polarized and its major axis rotates slightly.

Under these conditions, the complex Kerr angle is given by Relation [42]:

$$\frac{1+\tan\gamma_k}{1-\tan\gamma_k} e^{i2\theta_k} = \frac{(1+n_+)(1-n_-)}{(1-n_+)(1+n_-)} \quad (4)$$

where

θ_k −Kerr rotation.

γ_k − ellipticity of Kerr.

$n_{\pm}^2$ − eigenvalues of tensor $\sigma(\omega)$ represented by the equation

$$n_{\pm}^2 = 1 + \frac{4\pi i}{\omega} + \left(\sigma_{xx} \pm \sigma_{xy}\right) \quad (5)$$

Because θ_k and γ_k are usually less than one degree for most materials, we can express them in the form

$$\theta_k + i\gamma_k = \frac{-\sigma_{xy}}{\sigma_{xx}\sqrt{1+\left(\frac{4\pi i}{\omega}\right)\sigma_{xx}}} \quad (6)$$

To explore the magneto-optical response of PdM alloys (M = Fe, Co, Ni), we computed the P-MOKE spectra of the systems over a wide energy range up to 9 eV. The Kerr magneto-optical rotations are illustrated in Fig. 8.

The spectra exhibit a negative peak in the visible range. Specifically, in the case of the PdFe system (Fig. 8), two negative peaks are observed: the first at E = 2.20 eV and the second at E = 5.747 eV with θ_k= -0.18°, -0.28°, respectively. In contrast, the PdCo system [Fig. 8(c)] is characterized by a single negative peak (-0.28°) at E = 5.28eV.

However, the PdNi system [Fig. 8(b)] shows a unique positive peak of 0.39° at E = 0.52 eV.

We were satisfied with a qualitative explanation of interband transitions between localized states only. For this, we calculated the densities of states which are illustrated in Fig. 9.

a)

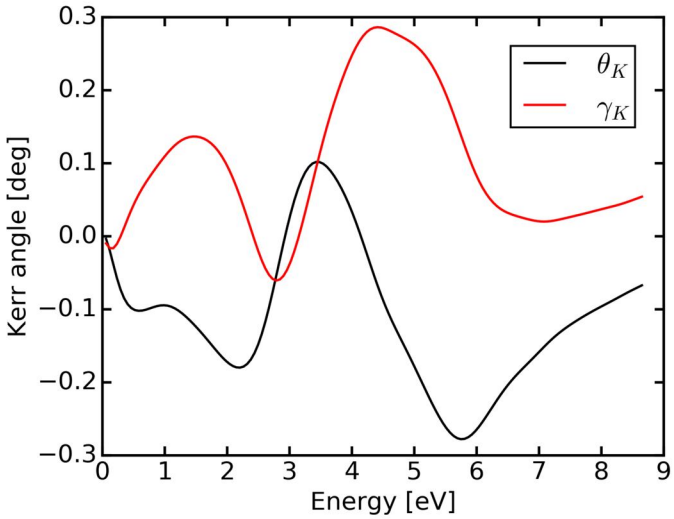

b)

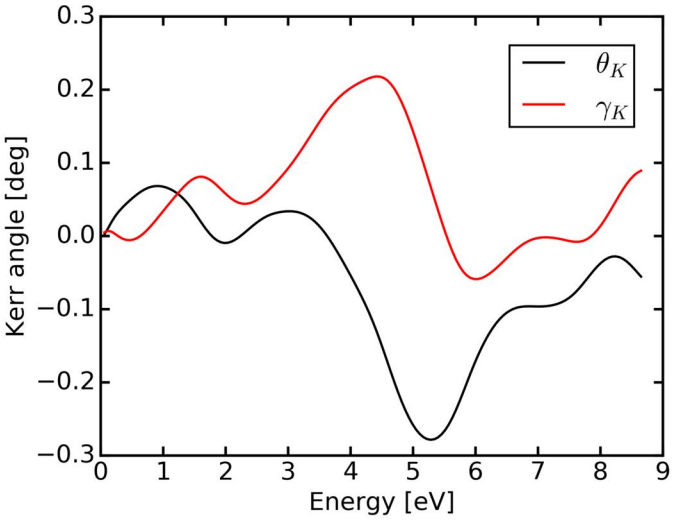

c)

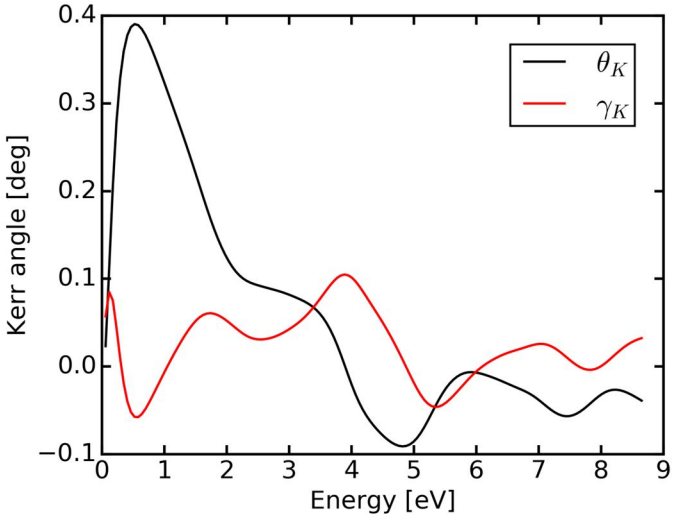

FIG. 8. Kerr spectrum of: (a) PdFe, (b) PdCo, (c) PdNi.

a)

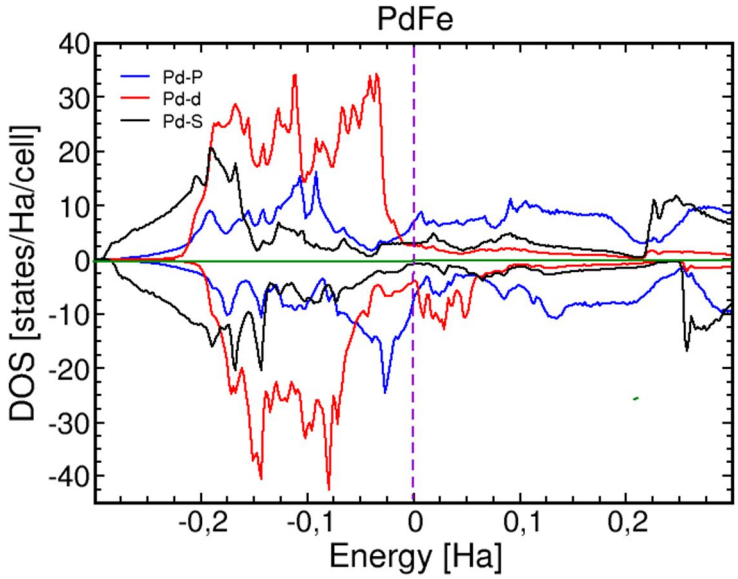
PdFe
Pd-P
Pd-d
Pd-S
DOS [states/Ha/cell]
Energy [Ha]

b)

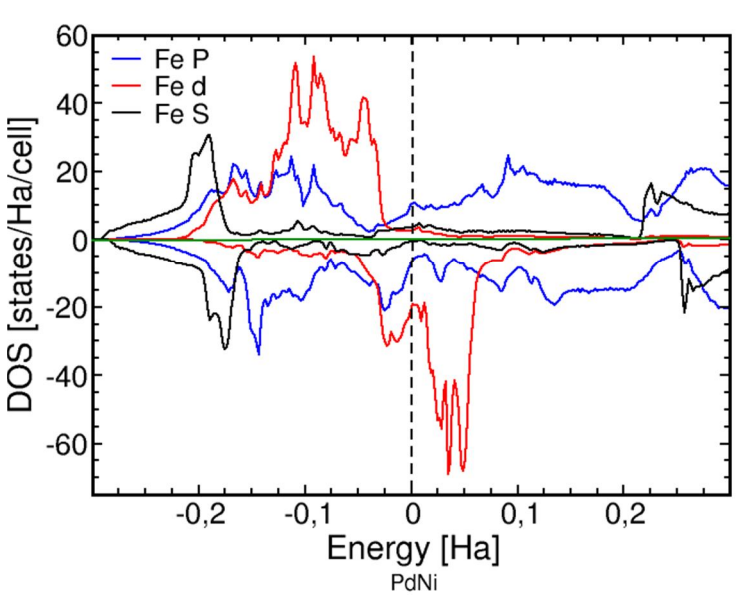
PdFe
Fe P
Fe d
Fe S
DOS [states/Ha/cell]
Energy [Ha]

c)

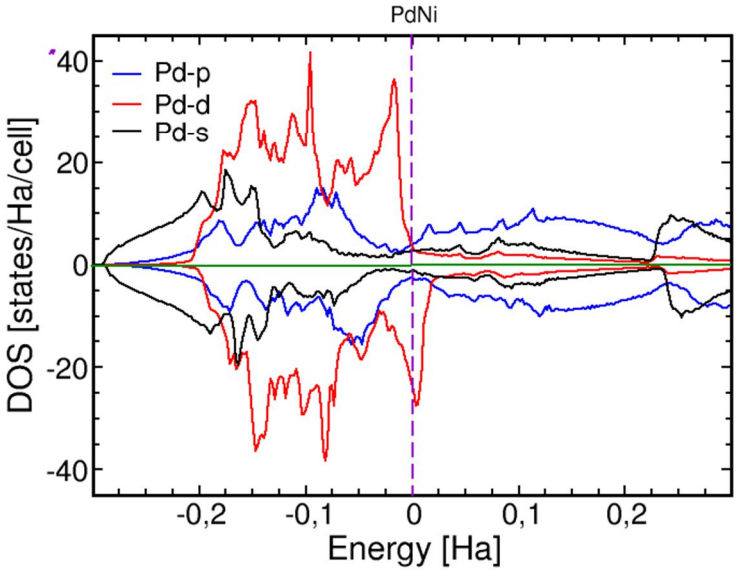
PdNi
Pd-p
Pd-d
Pd-s
DOS [states/Ha/cell]
Energy [Ha]

d)

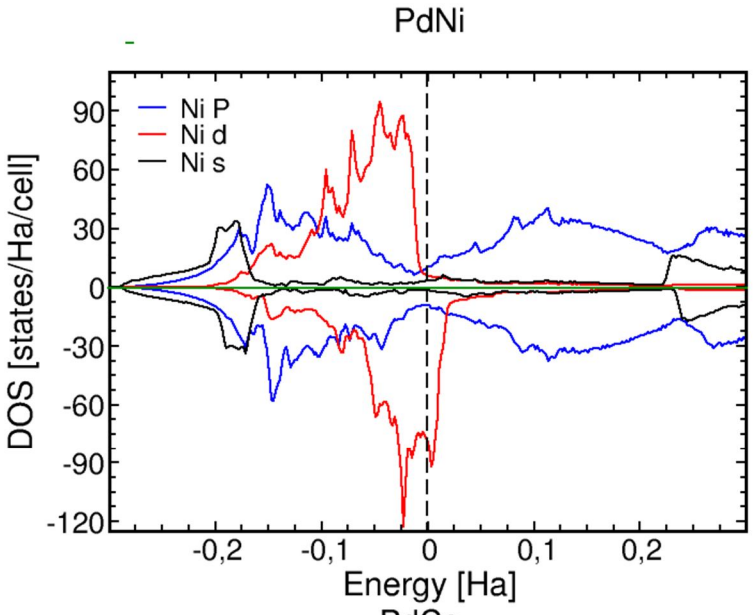

e)

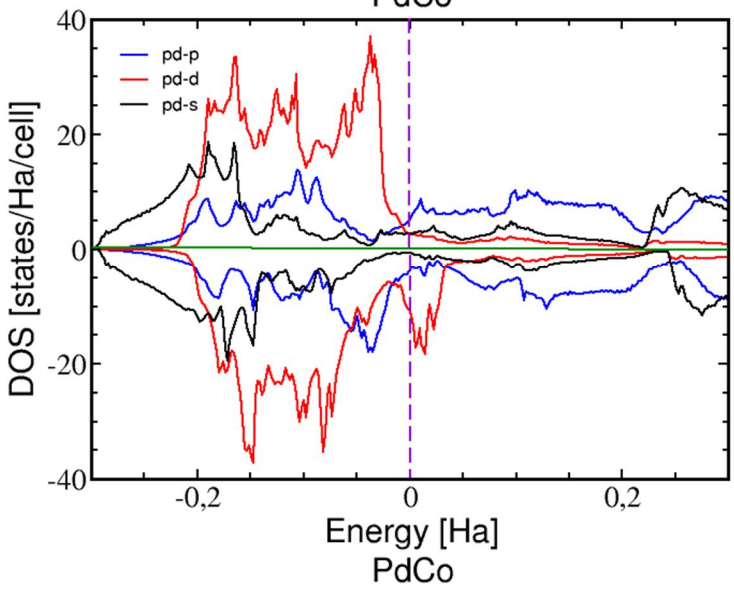

f)

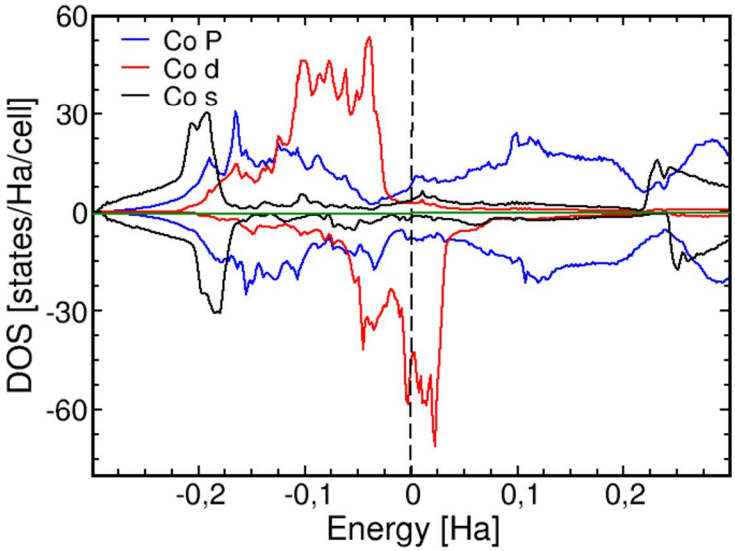

FIG. 9. Partial densities of states in the system (a), (b) PdFe, (c), (d) PdNi, (e), (f) PdCo (states and p are multiplied by a factor of 10).

According to Fig. 9, the PDOS analysis from PdNi, it follows that the lowest-energy interband transitions in the region E < 1 eV are associated with d → d and p → d transitions in the spin band↓. In the energy region E = 4 eV, interband d → p transitions exist in both spin subbands, PdFe and PdCo. In the subzone↑, we see the possibility of d →p interband transitions with a maximum in the region of 4 eV and almost no interband transitions in the region of E < 1 eV. In the energy region E = 4-6 eV, interband d → s transitions exist in both spin subbands. The competition of these transitions determines the behavior of P-MOKE in the high-energy region.

The magnetic properties of the different systems studied come from the d states.

The most prevalent inter-band transitions which participate in Kerr rotations and ellipticities are shown in the following table.

TABLE 4. Interband transitions for the PdM alloy (M = Fe, Co, Ni).

	θ_k	γ_k	transition
PdFe	-0.18° (2.20eV) -0.28° (5.74eV) 0.10°(3.42eV) -0.26° (4.9eV)[a]	0.14°(1.45eV) 0.28° (4.41eV) 0.22° (2.55eV)[a]	d↓→ p↓ s↓→ d↓
PdCo	-0.28° (5.28 eV) -0.22°(4.7eV)[a]	0.22° (4.41eV) 0.18° (2.5eV)[a]	s↓→ d↓
PdNi	0.39° (0.52 eV)	-0.49° (0.0583 eV) 0.105°(3.9eV)	d↓→ d↓ p↓→ d↓

a: Expt : [40].

The main characteristic of the magneto-optical properties in the PdM system (M = Fe, Co, Ni) is a positive peak in the visible range with appreciable angles of rotation. The inter-band transitions that underlie these rotations take place between localized states in the absence of spin-flip.

4. Conclusion

In the investigation of the structural properties of PdM alloys (M = Fe, Co, Ni), our results demonstrate reasonable agreement with experimental data and other theoretical findings available in the literature for all systems.

The second step was to study the magnetic properties of our alloys. The analysis through total state densities (TDOS) and partial state densities (PDOS), has shown metallic behavior for PdM (M = Fe, Co, Ni) with ferromagnetic coupling. The magnetic moments obtained from these alloys are in good agreement with the experimental results. According to the curves obtained, the magnetic properties of the different systems studied come from the d states.

We were particularly interested in the study of the magneto-optical Ker effect in its polar geometry by calculating the spectra of Kerr rotations and ellipticities as functions of incident photon energies. We found in the PdFe systems two negative peaks: the first at E = 2.20 eV (-0.18°) and the second at E = 5.74 eV (0.28°), while PdCo displays a negative peak at E = 5.28ev (-0.28°). In contrast, the PdNi system has a single positive peak at E = 0.53 eV (0.39°).

To explain the microscopic origin of the peaks appearing in the spectra of Kerr rotations and ellipticities, a qualitative projection analysis of partial densities of states was performed. The dominant interband transitions identified for all systems are d → p and s → d in spins down. These findings are compared with other studies.

Acknowledgments

This work was supported by the Algerian Ministry of Higher Education and Scientific Research.

References:

[1] Rehan Ullah, M.A.A., J. Magn. Magn. Mater., 546 (2022) 168816.

[2] Rehan Ullah, M.A.A., J. Solid State Chem., 293 (2021) 121823.

[3] Rehan Ullah, M.A.A., Mat. Sci. Semicon. Proc., 137 (2022) 106218.

[4] Kamde, S.N., Nandanwar, A.K., Agone, P.G. and Rewatkar, K.G., Jordan J. Phys., 15 (1) (2022) 57.

[5] Oboz, M. and Śniadecki, Z., J. Magn. Magn. Mater., 511 (2020) 167000.

[6] Westbrook, J.H. and Fleischer, R.L., "Intermetallic Compounds", (John Wiley & Sons, Vol.3: Progress, Chichester, 2002).

[7] Sauthoff, G., "Intermetallics", (Wiley-VCH, Weinheim, 1995).

[8] Benamara, O. and Boufelfel, A., J. Supercond. Nov. Magn., 29 (2016) 1013.

[9] Meyer, E. and Taziwa, R., Metals, 9 (2019) 796.

[10] Matin, Md.A. and Jang, J.-H., J. Power Sources, 262 (2014) 356.

[11] Shima, H., Oikawa, K., Fujita, A., Fukamichi, K., Ishida, K. and Sakuma, A., Phys. Rev. B, 70 (2004) 224408.

[12] Senoussi, S. and Campbell, L.A., Solid State Commun., 21 (1977) 269.

[13] Taylor, J.W., Duffy, J.A. and Poulter, J., Phys. Rev. B, 65 (2001) 024442.

[14] Van Acker, J.F., Speier, W. and Zeller, R., Phys. Rev. B, 43 (1991) 9558.

[15] Parra, R.E. and Gonzalez, A.C., J. Appl. Phys., 75 (1994) 7137.

[16] Kakeshita, T. and Ullakko, K., MRS Bull., 27 (02) (2002) 105.

[17] Mansuripur, M., "The Physical Principles of Magneto-Optical Recording", (Cambridge University Press, Cambridge, England, 1995).

[18] Zeeman, P., Leiden. Commun., 15 (1895).

[19] Martın-Gonzalez, M.S. and Huttel, Y., Surf. Sci., 571 (2004) 63.

[20] Takahashi, H., Tsunashima, S. and Fukatsu, S., J. Magn. Magn. Mater., 93 (1991) 469.

[21] Visnovsky, S., Kielar, P. and Nyvlt, M., JEEE Transmagnetics, 29 (1993).

[22] Hohenberg, P. and Kohn, W., Phys. Rev., 136 (1964) B864.

[23] Kohn, W. and Sham, L.J., Phys. Rev., 140 (A1) (1965) 133.

[24] Gulans, A., Kontur, S. and Meisenbichel, C., J. Phys. Condens. Matter., 26 (2014) 363202.

[25] Perdew, J.P., Burke, K. and Ernzerhof, M., Phys. Rev. Lett., 77 (1996) 3865.

[26] Birch, F., Phys. Rev., 71 (1947) 809.

[27] Mehaddene, T., Kentzinger, E., Hennion, B. and Tanaka, K., Phys. Rev. B, 69 (2) (2004) 024304.

[28] Al-Ghaferi, A., Mullner, P. and Heinrich, H., Acta Mater., 54 (4) (2006) 881.

[29] Halley, D., "Croissance mise en ordre chimique et relaxation des alliage Pd Fe. PdPt", (Université Joseph-Fourier – Grenoble, 2001).

[30] Boufelfel, A., Int. J. Hydrogen Energ., 41 (8) (2016) 4719.

[31] Ghosh, S., J. Phys. Condens. Matter., 20 (27) (2008) 275208.

[32] Bourezg, A., "Propriétés physiques des couches minces de Co100-x Pdx élaborées sous vide par évaporation thermique", (Université Ferhat ABBAS Sétif1, 2018).

[33] Sadhukhan, B., Nayak, A. and Mookerjee, A., Comp. Mater. Sci., 140 (2017) 1.

[34] Durga, P. and Abhijit, M., J. Phys. Condens. Matter., 16 (2004) 5791.

[35] Wang, L.G. and Zunger, A., Phys. Rev. B, 67 (2003) 092103.

[36] Arejdal, M. and Kadiri, M., J. Supercond. Nov. Magn., 29 (2016) 2659.

[37] Arejdal, M. and Bahmad, L., J. Physica A, 437 (2015) 375.

.[38] Wijn, H.P.J., "Data in Science and Technology", (Springer, Berlin, 1991).

[39] Kashyap, A., Skomski, R. and Solanki, A.K., J. App. Phys., 95 (2004) 11.

[40] Yaresko, A.N., Uba, L., Uba, S. and Ya, A., Perlov. Phys. Rev. B., 58 (1998) 12.

[41] Martin, D.H., Neal, K.F. and Dean, T., J. Proc. R. Soc., 86 (1965) 605.

[42] Reim, W. and Schoenes, J., "Ferromagnetic Materials" Eds. E.P. Wohlfarth and K.H.J. Buschow, (North-Holland, Amesterdam, 1988), vol. 4, p.588.